

## A First Principles Study of Substitutional Copper in Aluminium

A.E. Smith, S. Homolya

School of Physics and Materials Engineering, Monash University, Victoria, 3800, Australia

Keywords: Computer simulations, First Principles, Aluminium alloys

### Abstract

This study aims to gain insight into the early stages of precipitation hardening by determining the energetics of atom replacement by first principles computations. Density functional theory calculations using the ABINIT code were performed to determine cohesive energies and the equilibrium lattice constants of aluminium and copper for the conventional face centred cubic structure of 4 atoms. These were extended to periodic super cells of different cubic geometries and with primitive cell size of up to 32 atoms with replacement of a single aluminium atom by copper.

### 1. Introduction

The aluminium - copper alloy system has been the subject of much computer modelling. Most simulations employ semi-empirical methods, using system specific parameterisations, often in terms of interatomic potentials [1-3]. However, considerable progress has been achieved using so-called first principles methods in which the numerical schemes are formulated within the framework of quantum mechanics with minimal parameterisation [4,5]. This paper employs one such first principles method to investigate the substitution of copper into aluminium.

### 2. Method

#### 2.1. Model Systems

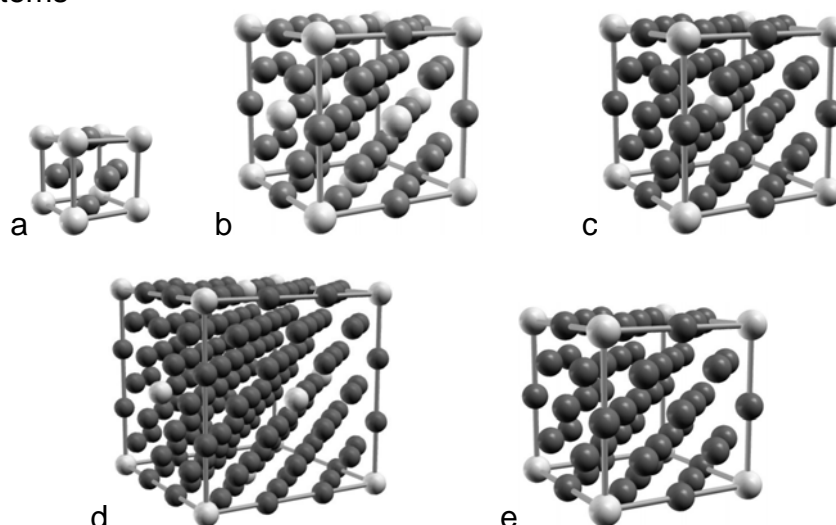


Figure 1: Unit cells used to study substitutional copper (light coloured balls) in face-centred cubic aluminium (dark coloured balls). Illustrations were generated using the XCrysDen program [6].

Substitutional properties of copper in aluminium were investigated using the pure metallic face-centred cubic (fcc) structures compared with the periodic structures illustrated by the unit cells shown in Figure 1. These consist of collections of fcc aluminium cells, where selected aluminium atoms are replaced with copper.

In all five structures, all copper atoms occupy equivalent sites within the bulk solid, i.e., sites of simple cubic [Figures 1(a) and 1(e)], body-centred cubic [Figure 1(c)] and fcc [Figures. 1(b) and (d)] lattices respectively.

Such regular arrangements of atoms are clearly idealisations of real dilute solid solutions where solute atoms would occupy sites at random (before any clustering or precipitate formation). However, the periodicity of the model systems permits the determination of observable properties of the solids by the use of Bloch formalism together with tractable approaches to the fundamental laws of quantum mechanics that govern the interaction between nuclei and electrons.

## 2.2. Frozen Core Approximation

Structural properties were determined by minimising the total energy of the system with respect to atomic positions and unit cell geometry. This was carried out by first performing electronic calculations for fixed atomic positions within the Born-Oppenheimer approximation [2], where the slow motion of heavy nuclei are decoupled from the motion of electrons. Furthermore, for the calculation of the electronic structure of the solids, the present study employs the frozen core approximation in which the valence electrons are considered to move in a static background potential due to Coulomb interaction with frozen nuclei and frozen core electrons, which are tightly bound to nuclei. Accordingly it is only the valence electrons that participate in chemical bonds and determine the nano-structure of the solid. Aluminium atoms were modelled using a neon-like frozen core with three valence electrons and copper by an argon-like core with 11 valence electrons.

## 2.3. Density Functional Theory

Electronic structure of the solids was computed within the framework of density functional theory (DFT) [8,9]. The advantage of DFT over other ab initio methods is that it efficiently describes all observable properties of the system in its ground state in terms of the electronic charge density, rather than the computationally intractable many-body wavefunction. The charge density is determined by solution of the Kohn-Sham (KS) equations for single-particle-like wavefunctions or orbitals [9]. These orbitals are analogous to the one electron orbitals in the non-interacting approximation, except that the potential term in the KS equations depends on the orbitals themselves. Thus the equations must be solved iteratively, until a self-consistent solution is found. After this process is completed and to determine the equilibrium or stress-free structure, the total energy of the system needs to be minimised numerically with respect to atomic positions and unit cell geometry.

For the present study, the KS equations were solved using the ABINIT software package [10]. The code is able to determine the electron density and related properties, including total energy, forces on nuclei, and internal stress due to non-equilibrium unit cell geometry. The latter two are utilised by the code in searching for the energy minimised, relaxed, crystal structure. The frozen atom cores are modelled using the norm-conserving pseudopotential (PSP) approximation, which allows the projection of the Kohn-Sham orbitals on to a computationally efficient orthogonal plane wave basis set. The pseudopotentials for aluminium and copper were generated using the FHI98PP [11].

While DFT can be considered an exact theory, its practical application requires the use of a numerical approximation to the exchange correlation functional (XCF) which describes the many-body quantum interaction between electrons. For the present study, the Perdew-Burke-Ernzerhof generalised gradient approximation (GGA) [12] was used for the XCF.

## 2.4. Numerical Accuracy

Key parameters that determine the quality of the numerical results are the length  $L_k$  of shortest supercell vector, the Fermi level smearing parameter  $E_{\text{tsm}}$ , and the kinetic energy cut-off  $E_{\text{cut}}$ . As input and/or output variables for the ABINIT code, these parameters are denoted by identifiers `kptrlen`, `tsmear` and `ecut`, respectively. We give a brief description of the role of these variables in the following.

Parameter  $L_k$  is the size of the bounding box over which periodic boundary conditions are imposed on the wave function. The bounding box contains an integral number of primitive unit cells, equal to the number of distinct Bloch wavevectors  $\mathbf{k}$  [13] for which the KS equations must be solved.  $L_k$  needs to be sufficiently large so that the computational model is a good approximation to the macroscopic solid. In practical terms this means that physical quantities of interest are converged with respect to  $L_k$ .

As we are dealing with metallic systems, the valence and conduction bands overlap, and the number of occupied orbitals is  $\mathbf{k}$ -dependent. Consequently, the total energy is not a smooth function of other physical properties of the system and computational parameters. To avoid numerical instabilities this can lead to, a smearing of the occupation numbers near the Fermi level is applied using a smearing window of width  $E_{\text{tsm}}$  [14]. If the smearing parameter is too large, however, the accuracy of the results may be compromised.

Finally, the maximum kinetic energy  $E_{\text{cut}}$  of the KS quasi-particles is used to limit the size of the plane wave basis set on which the wavefunctions are expanded. For a given unit cell, this parameter usually dominates the computational complexity of the problem.

## 3. Results and Discussion

### 3.1. Convergence of Total Energy and Lattice Geometry

To ensure adequate numerical accuracy in the results, convergence studies were carried out for the pure metals and for the smallest binary system  $\text{Al}_3\text{Cu}$  [Figure 1(a)] with four atoms per unit cell. Figure 2 shows results for the convergence of calculated energies with respect to parameters  $E_{\text{cut}}$  and  $L_k$ .

The energy of formation of the binary alloy from pure metals is determined by energy differences between the relaxed binary structure and the pure metals. It is plotted as a function of  $E_{\text{cut}}$  in Figure 2(a) for fixed  $L_k = 56 \text{ \AA}$  and  $E_{\text{tsm}} = 0.54 \text{ eV}$ . The results indicate that  $E_{\text{cut}} > 1000 \text{ eV}$  is adequate for an accuracy of about  $0.01 \text{ eV}$ , and for  $E_{\text{cut}} > 1200 \text{ eV}$  the uncertainty is less than  $0.001 \text{ eV}$ . These results may be extended to larger unit cells by recognising that the numerical error in the energy of formation can be expected to scale linearly with the number of atoms in the unit cell. Analogous results for the unit cell geometries indicate less than  $0.004 \%$  numerical error in the lattice parameter for  $E_{\text{cut}} > 1000 \text{ eV}$ .

Figure 2(b) shows how the calculated value of the total energy per unit cell of  $\text{Al}_3\text{Cu}$  depends on the size  $L_k$  of the system, for selected values of  $E_{\text{tsm}}$  and a fixed  $E_{\text{cut}} = 1088 \text{ eV}$ . The data show that at  $E_{\text{tsm}} = 0.04 \text{ Ha} = 1.09 \text{ eV}$ , the smearing of the Fermi level is excessive and dominates numerical errors in the limit of large system size, while

for  $E_{\text{tsm}} < 0.6$  eV, the accuracy is good, with errors less than about 0.001 eV for  $L_k > 50$  Å. Uncertainty in lattice parameters is also small in this regime, less than 0.004 %. Quantitatively similar results were obtained for pure copper, while numerical errors are about an order of magnitude smaller for the free-electron-like pure aluminium.

On the basis of these convergence tests the results presented below were obtained with  $E_{\text{cut}} = 1224$  eV,  $E_{\text{tsm}} = 0.27$  eV and  $L_k > 60$  Å.

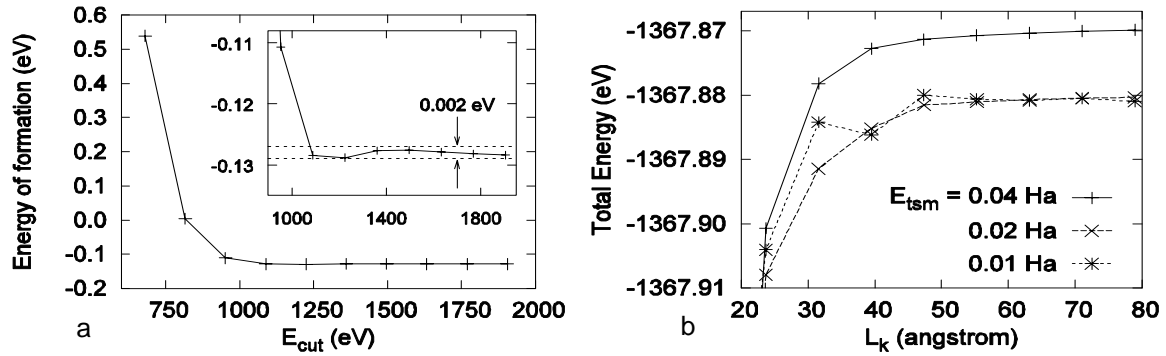


Figure 2: Convergence of numerical results with respect to computational parameters. (a) Plot of energy of formation per unit cell of  $\text{Al}_3\text{Cu}$  [Figure 1(a)] from pure metals against kinetic energy cut-off  $E_{\text{cut}}$ . Inset shows detail for large values of  $E_{\text{cut}}$ . (b) Plot of total energy per unit cell of  $\text{Al}_3\text{Cu}$  as a function of numerical system size  $L_k$ , for three values of Fermi level smearing window width  $E_{\text{tsm}}$  (1.00 Ha = 27.2 eV).

### 3.2. Energy of Formation of Binary Alloys from Pure Solids

Results for the energy of formation  $E_{\text{form}}$  per primitive unit cell, i.e., per copper atom, from pure metals are shown in Tab. 1, for the five structures shown in Figure 1. For all cases, the data show the reaction  $n \text{Al} + \text{Cu} \rightarrow \text{Al}_n\text{Cu}$  to be energetically favourable, with  $E_{\text{form}} < 0$ . At copper concentrations of 1 in 16 atoms or less the energies of formation are consistent within numerical error, indicating a heat of solution of about -0.13 eV per atom for copper in aluminium. This agrees with the experimentally derived value [15]. However, it is well known that care must be taken when high temperature experimental data is used in comparison with zero temperature calculations and zero concentration properties are extrapolated from those at finite values [16]. At a copper concentration of 1 in 8 atoms the energy of formation is calculated to be -0.18 eV, indicating a significant energy contribution from the interaction between copper atoms that is not present in the dilute limit.

Table 1: Calculated energy of formation  $E_{\text{form}}$  per primitive unit cell of model solids  $\text{Al}_n\text{Cu}$ , shown in Figure 1, from pure metals.

$n$	3	7	15	26	31
$E_{\text{form}}$ (eV)	-0.130(1)	-0.180(2)	-0.129(4)	-0.135(7)	-0.127(8)

### 3.3. Effect of Copper Concentration on Lattice Geometry

Table 2 shows our results for the relaxed geometries of the Al-Cu systems and for pure metals, as well as experimental values for solid solutions of copper in aluminium and the pure metals [17,18].

For pure aluminium, the agreement between theory and experiment is excellent, with an error of about 0.1% in the theoretical value of the lattice parameter. The discrepancy is much larger for copper, however, at about 2 %. This is attributable to increased errors in the GGA and the frozen core PSP approximation in the presence of rapid spatial variations of the electronic charge density associated with the 3d orbitals of the transition metal.

For the model systems shown in Figure 1(a) and (b), with four and eight atoms in the primitive unit cell, respectively, geometry optimisation resulted in a uniform contraction of the crystal lattice. The fcc structure of the host lattice was retained due to symmetry. The contraction of the lattice corresponds to a decrease in lattice parameter by 2.4 % for  $\text{Al}_3\text{Cu}$  and 1.2 % for  $\text{Al}_7\text{Cu}$  (see Tab. 2). For the three larger unit cells with lower copper concentrations [Figures 1(c)-(e)], the fcc structure of the aluminium host lattice was found to be significantly perturbed by the presence of substitutional copper. The strain was found to be greatest near copper atoms, with a consistent reduction of separation between copper and nearest-neighbour aluminium atoms by 1.5 %, while the overall contraction of the lattice was smaller, at roughly 0.5 %. Table 2 shows the mean lattice parameters for the periodic solids, defined in terms of the change in volume of the unit cell.

Table 2: Present (theoretical) and experimental results for the lattice parameter of Al-Cu alloys and the pure metals.

	atom % Cu	lattice parameter (Å)	
Binary alloys	25.0	3.9436(2)	Theoretical
	12.5	3.9908(2)	
	6.25	4.0208(2)	
	3.7037	4.0307(2)	
	3.125	4.0330(2)	
	1.62	4.0335(5)	Experimental [17]
	1.37	4.0347(8)	
Pure metals	0.00 (pure Al)	4.0465(1)	Theoretical
		4.0413(4)	Experimental [17]
	100.0 (pure Cu)	3.6777(2)	Theoretical
		3.6149(1)	Experimental [18]

To better facilitate comparison between theory and experiment, we have calculated the relative change,  $\langle a \rangle / a_{\text{Al}}$ , in mean lattice parameter  $\langle a \rangle$  compared with the lattice parameter  $a_{\text{Al}}$  of pure aluminium. The data are plotted in Figure 3, and show good agreement between theoretical and experimental results.

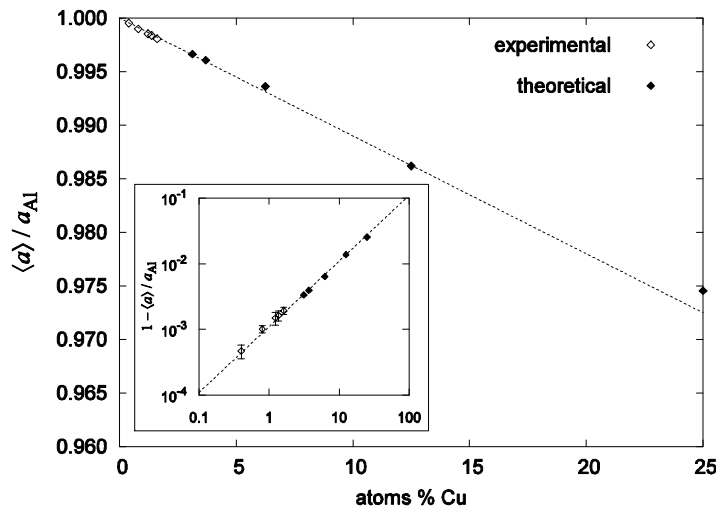


Figure 3: Comparison of experimental [17] and theoretical results for the relative change in lattice parameter of aluminium, after the introduction of substitutional copper. Symbols  $\langle a \rangle$  and  $a_{\text{Al}}$  denote the mean lattice parameter for the binary alloy and for pure aluminium, respectively.

## 4. Conclusions

First principles computational studies of substitutional copper in aluminium were carried out. The energy of formation of periodic solids with primitive unit cells containing one copper and up to 31 aluminium atoms indicates a heat of solution of - 0.13 eV for copper in aluminium. Theoretical results for the change in the volume of the bulk solid as a function of copper content show good agreement with experiment.

## Acknowledgements

Computations were performed at the HPC facilities of the Victorian Partnership for Advanced Computing <http://www.vpac.org> (Expertise Grant Scheme) and the Australian Partnership for Advanced Computing <http://www.apac.edu.au> (Merit Allocation Scheme).

## References

- [1] C. Lane Rohrer, *Modelling Simul. Mater. Sci. Eng.*, 2, 119-134, 1994.
- [2] M. Widom, I. Al-Lehyani and J.A. Moriaty, *Phys. Rev. B* 62, 3648-3657, 2000.
- [3] G. Bozzolo et al., *Comput. Mat. Sci.*, 15, 169-195, 1999.
- [4] C. Wolverton, *Acta Mater.*, 49, 3129-3142, 2001.
- [5] T. Hoshino et al., *Comput. Mat. Sci.*, 14, 56-61, 1999.
- [6] A. Kokalj, *J. Mol. Graphics Modelling*, 17, 176, 1999. See also <http://www.xcrysden.org>.
- [7] G.D. Mahan, *Many-Particle Physics*, 3<sup>rd</sup> edn., Kluwer Academic/Plenum Publishers, 2000, p. 27.
- [8] P. Hohenberg and W. Kohn, *Phys. Rev.*, 136, B864-B871, 1964.
- [9] W. Kohn and L.J. Sham, *Phys. Rev.* 140, A1133-A1138, 1965.
- [10] X. Gonze et al, *Comput. Mat. Sci.*, 25, 478-492, 2002. (The ABINIT code is a common project of the Université Catholique de Louvain, Corning Incorporated, and other contributors. See <http://www.abinit.org>.)
- [11] M. Fuchs, M. Scheffler, *Comput. Phys. Commun.*, 119, 67-98, 1999.
- [12] J.P. Perdew, K. Burke, and M. Ernzerhof, *Phys. Rev. Lett.*, 77, 3865-3868, 1996.
- [13] C. Kittel, *Introduction to Solid State Physics*, 4<sup>th</sup> edn., John Wiley & Sons, 1971, pp. 299-310.
- [14] N. Marzari et al., *Phys. Rev. Lett.*, 82, 3296-3299, 1999.
- [15] R. Hultgren et al., *Selected Values of the Thermodynamic Properties of Binary Alloys*, American Society for Metals, 1973, p. 154.
- [16] G.J. Ackland and V. Vitek, *Phys. Rev. B* 41, 10324-10333, 1990.
- [17] H.J. Axon and W. Hume-Rothery, *Proc. Royal Soc. Lond. A*, 193, 1-24, 1948.
- [18] M. E. Straumanis and L. S. Yu, *Acta Crystallogr.*, 25A, 676-682, 1969.